

# Real-time all-optical quality of service monitoring by use of correlation and a network protocol to exploit it

Betty Lise Anderson, Arjan Durreesi, David Rabb, and Feras Abou-Galala

We propose to use optical correlation to measure the quality of an optical link in real time, staying completely within the optical domain. We transmit a test signal of 010 and correlate the received (degraded) signal with 010. The strength and shape of the output measure dispersion and attenuation in just 3 bit periods (75 ps at 40 Gb/s) compared with minutes by traditional methods. Correlation becomes feasible owing to the recent development of tapped delay lines with very large numbers of taps. We present simulations showing that this technique can detect attenuation, dispersion, noise, and jitter. With this instantaneous quality-of-service information available to all nodes in a network, new protocols will enable the network to select paths based on quality, allowing service providers to take into account the system's physical impairments when selecting new light paths or when restoring existing ones and to guarantee varying levels of service. We present one such protocol. © 2004 Optical Society of America

*OCIS codes:* 060.2230, 070.0550, 060.0250.

## 1. Introduction

When a bit stream is sent over a fiber optic link, it undergoes degradation due to attenuation, dispersion, noise, and jitter, among other things. As the shape and amplitude of the bits change, the receiver's ability to reliably distinguish 1s from 0s is also reduced. In current technology the degree of degradation is typically measured by sending a pseudorandom bit stream over a link and comparing the receiver's best guess for each bit with the original signal. At a typical phone-line bit error rate (BER) of  $10^{-9}$ , a billion bits must be received, on average, before a single error is detected, and usually at least 100 errors are required ( $10^{11}$  bits) for the measurement to be statistically significant. For data links BERs of  $10^{-12}$  are not uncommon and require  $10^{14}$  bits, or  $\sim 40$  min at the fastest bit rate (40 Gb/s). For more typical links measurement can take more than an hour. Furthermore, BER measurements require disrupting the data stream to send a lengthy

known bit sequence. Eye diagram measurement may be faster and can be performed on real-time data, but again requires the reception of many bits in order to form a significant sample and still requires the conversion of the optical signal to an electronic one.

Thus both BER and eye-diagram measurement processes are slow because of the optical-to-electronic conversion and the requirement that huge numbers of bits be collected. At present the only thing that can be detected instantly is a complete loss of signal. In dynamically reconfigurable networks, however, dispersion changes with each reconfiguration, and other parameters may fluctuate as well. Thus it is essential to obtain quality measurements in a very short time so that the network can respond to the changes.

Here we propose a completely new method to monitor the health of a link, one that produces results in real time. This method is based on optical correlation, comparing received degraded signals with undegraded ones. For example, one sends a test sequence (at the normal bit rate) of 010. The received signal exhibits the cumulative effects of attenuation, dispersion, noise, and jitter. One then correlates the received signal with an unimpaired 010. The output of the correlator is an optical pulse, whose amplitude and shape directly measure the degree to which the degraded and undegraded signals are similar. The optical pulse can be thresholded or integrated optically to generate a control signal (ei-

---

B. L. Anderson (anderson@ee.eng.ohio-state.edu), D. Rabb, and F. Abou-Galala are with the Department of Electrical Engineering, Ohio State University, 205 Dreese Laboratory, 2015 Neil Avenue, Columbus, Ohio 43210. A. Durreesi is with the Department of Computer and Information Science, Ohio State University, 365 Dreese Laboratory, 2015 Neil Avenue, Columbus, Ohio 43210.

Received 26 March 2003; revised manuscript received 4 November 2003; accepted 4 November 2003.

0003-6935/04/051121-10\$15.00/0

© 2004 Optical Society of America

ther optical or electrical) for switches or other devices, or it can be detected and used to set software flags.

We emphasize that this does not entail sending and detecting a code, or sending a bit stream and detecting whether the same bits are detected. In this approach the test signal is treated entirely as an analog test signal. The correlation measures change according to the shape of the signal.

This kind of optical signal processing requires an optical correlator with very high resolution, which has not been available until recently. This is because a correlator's key element is a tapped delay line, and the performance of high-resolution correlation requires hundreds or thousands of taps. That is, the (effectively analog) test signal should be sampled with very high resolution. Fiber-based tapped delay lines are not expected to exceed 100 taps. A free-space programmable optical delay line with more than 6,000 delays was recently reported.<sup>1</sup> Because the delays are fixed this can be simplified to become a tapped delay line, making high-resolution optical (temporal) correlation feasible for the first time.

Once the quality of a given link can be known instantaneously, then each node in a network can keep track of the current quality of all its links. This calls for a new paradigm in network protocols that allows networks to route signals based not only on the existence of connections but also on their quality. Existing routing protocols through all-optical networks assume that all routes have adequate signal quality.<sup>2-5</sup> This may be ensured by limiting the geographic size of all-optical networks such that the signal is converted to electronics and is regenerated periodically. There are, however, strong reasons to consider all-optical networks in which not all routes have adequate signal quality. First, as the bit rates increase it is necessary to increase power. This makes impairments and nonlinearities more troublesome. Second, all-optical networks can serve more economically as express backbones for longer distances.

There is a strong interest in the industry that routing protocols in all-optical networks be able to account for the impairments of the optical layer.<sup>6,7</sup> It is also known that there are many types of physical impairment introduced by various components of an optical network. Evaluating theoretically such impairments would be very difficult, and thus being able to measure them easily and in real time would be valuable.

One would therefore like to take advantage of the quality-of-signal information made available by an optical correlation device in the design of a new routing and protection protocol. When selecting a route, the routing protocol checks that the quality of signal is acceptable. However, should the quality of the signal in the original route fall below the acceptable threshold, the protection will reroute the connection. The ultimate goals are to allow carriers to quickly and dynamically provision network resources by op-

timizing the revenues, the quality of service (QoS) and the network utilizations and to support network survivability by optimized mesh-based protection and restoration techniques.

The organization of this paper is as follows. In Section 2 we show how correlation can be used to measure QoS. In Section 3 we present simulations that compare the measured signal from a correlator with a figure-of-merit number based on the open area of the corresponding eye diagram. The network protocol is discussed in Section 4. Section 5 contains a discussion and a summary.

## 2. Correlation for Quality of Service

### A. Correlation Process

Optical correlators are well known and come in two basic styles: spatial and temporal. Spatial correlators take advantage of holograms, for example, to compare a two-dimensional image with some reference image (e.g., see Ref. 8). In temporal correlation a time-varying signal (e.g., intensity or phase) is correlated with a reference time-varying signal, using, for example, an acousto-optic device<sup>9-11</sup> or a fiber-optic tapped delay line.<sup>12-17</sup>

We propose to measure the quality of the optical link by using correlation by comparing the degraded, received bits with the known sent bits. One sends a short test signal (e.g., 010) over the link. At the opposite end, part of the energy of the received signal is split off and sent to the correlator.

In optical correlation the received signal  $r(t)$  is correlated in the optical domain with the sent signal  $s(t)$ , where  $t$  is time. The function

$$c(t) = \int_{-\infty}^{\infty} s(t)r(t - \tau)dt \quad (1)$$

is a measure of how similar  $r(t)$  and  $s(t)$  are. A correlation can be implemented in a discrete system by sampling the received signal  $N$  times, as<sup>18</sup>

$$c(t) = \sum_{k=0}^{N-1} s_k r(t - k\tau_k). \quad (2)$$

We use the discrete approach. Here the sent (reference) signal is represented as discrete weights  $s_k$ . They will be 1s and 0s in our case, given that we are correlating with a perfect 010. The received signal  $r(t)$  is replicated  $N$  times, and each duplicate is shifted in time by one increment, two increments, etc. Each time-shifted replica of  $r_k(t)$  is multiplied by a weight  $s_k(t)$ , and the resulting products are summed. The larger  $N$  is, the higher resolution the correlation and the more accurate the measurement.

A correlator is implemented physically as shown in Fig. 1. The received signal is sent to a tapped delay line. At each tap a small amount of the power is siphoned off. There is a time delay  $\tau$  between each tap. The signal replicas, which should all be of the same amplitude and are separated by a time  $\tau$ , are sent to weighting elements  $s_k$ . The weights can ei-

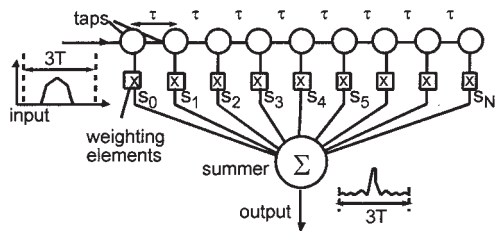


Fig. 1. Optical correlator based on a tapped delay line.

ther be phase shifters or amplitude weights or both. Let us suppose the  $s_k$  to be amplitude weights of either 1s or 0s. For light, this weighting can be accomplished with a shutter. Thus each time-shifted sample  $r(t - k\tau_k)$ , where  $t$  is time and  $\tau$  is the delay increment of the tapped delay line, is multiplied by the appropriate weight. These weighted and shifted replicas of the input signal are then summed. By using amplitude, rather than phase weights, the beams can be combined incoherently.

Let us select a node in a network and let it send the 3-bit-long signal depicted on the left-hand side of Fig. 2. The test signal can be sent between data packets, and the node can cycle through all its links, periodically slipping in these test signals, and thus monitor all the links in parallel with the same correlation hardware. After reception the signal is degraded. In the figure attenuation and dispersion are shown on the right-hand side.

As the signal propagates through the correlator, a replica of the signal is produced at each time interval  $\tau$ . Each of the replicas is multiplied by the appropriate weight, and finally they are all summed. The correlation function also occupies a time  $3T$ . If the two signals are identical, Eq. (2) becomes an autocorrelation, and the result appears as a single sharp peak in the center with low sidelobes, as shown in the lower right hand corner of Fig. 1. If the signals are less well matched, then the peak decreases and the information on either side of the peak increases.

The resolution, and therefore the quality, of the measurement depends on the number of taps available in the tapped delay line. For  $N$  taps the resolution of the correlation signal is generally  $N$ . For our case, however, half of the weights are zero, meaning that those copies of the signal that will be blocked need not be generated in the first place. Thus to achieve a resolution of  $N$  we require only  $N/2$  taps.

Correlators have been mentioned in the literature a great deal lately, primarily as encoders and decoders for optical code division multiple access.<sup>19–23</sup> A

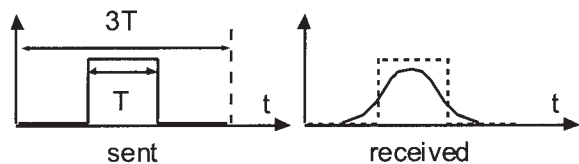


Fig. 2. Sent and received test signals.

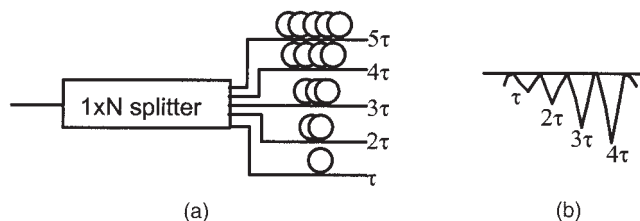


Fig. 3. Fiber-based tapped delay-line examples: (a)  $1 \times N$  splitter style and (b)  $2 \times 2$  coupler-splitter style

correlator is used to encode a bit stream with a chip code, with the entire code being repeated during each bit. A second correlator, with the order of the weights reversed, is used to decode the output. If the received chip code matches the one programmed into the correlator, a strong peak is observed in the optical output. This optical pulse can be used to drive optical switches to direct the signal to the correct destination. If there is no match, no strong peak is produced. Because it is all optical and because correlation is an inherently fast process, the decoding can take place in just picoseconds.

Correlators have other uses as well. The same hardware that makes a correlator can also be used for transversal filtering, which is in effect looking for a signal that matches a given expected signal. Optical correlators with real and complex weights can be used for a wide variety of signal processing functions.<sup>13,14,16,17,21,24,25</sup> Encryption can also be performed with correlation. The longer the length of the code, the better the encryption.

### B. Optical Correlator Based on the White Cell

Regardless of the application, the more taps the correlator has, the better. Optical taps for correlators are typically implemented with fiber splitters. Figure 3 shows two common styles. The tree in Fig. 3(a) consists of a  $1 \times N$  splitter followed by  $N$  lengths of fiber, each longer than the previous one,<sup>16–18,26</sup> and one in Fig. 3(b) uses  $2 \times 2$  coupler-splitters in various types of lattice.<sup>14,24,27,28</sup> The number of splitters is equal to the number of taps, and for each tap there is a separate, precisely cut optical fiber. Another recent approach uses fiber Bragg gratings.<sup>22,23</sup> In these applications a series of gratings in the fiber reflect back parts of the signal at different times, resulting in multiple replicas of the input signal space in time with the delay increment  $\tau$ . Superstructured fiber Bragg grating tapped delay lines with as many as 63 taps have been reported.<sup>29</sup>

Recently free-space programmable tapped delay lines were reported.<sup>1,30,31</sup> These use a series of White cells that share a common spatial light modulator (SLM) and that can produce thousands of delays or taps. The key characteristics of the White cell are that (a) large numbers of beams can circulate simultaneously (hundreds or thousands), (b) each beam forms a unique pattern of spots on the SLM so that each beam can be switched independently on each pass through the cell, and (c) the objective mirrors all

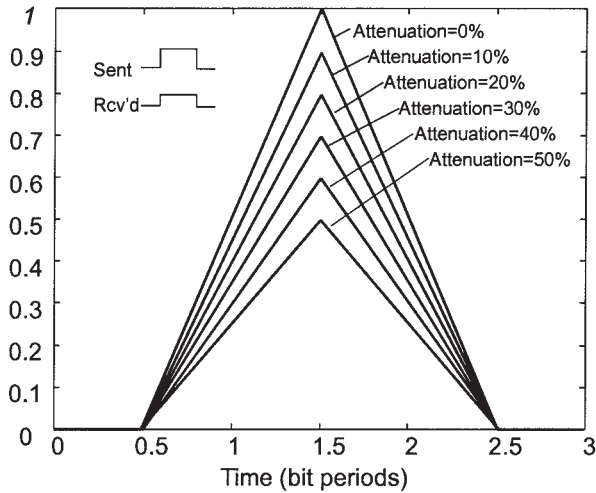


Fig. 4. Effect of attenuation on the correlation peak. Rcv'd = received signals.

image onto one another, thus eliminating diffraction losses. To implement time delays the SLM, which is either a liquid crystal or a micro-electromechanical systems (MEMS) mirror array, is used to switch each beam between White cells of varying lengths, thus changing the overall transit time through the device. These designs are best suited for intensity (incoherent) correlation, as opposed to complex (field and phase), coherent types of correlation.

For a tapped delay line, however, one does not need programmability and therefore does not need a SLM or a switch. Although a tip-style MEMS micromirror array was used in Refs. 1 and 31, for a tapped delay line, the MEMS can be replaced with a fixed micromirror array. For example, one might fabricate a set of microprisms by using reactive ion etching or another technique and then coat the entire array with a high-reflectivity coating. If each micromirror has a tip angle of north, south, east, west, or flat, then a given light beam can be made to have any of 6,399 different delays with only 17 round trips through the cell.<sup>1</sup> This is a factor of 100 improvement in the number of taps over existing tapped delay lines. Further, one can have hundreds or thousands of beams circulating in the same device, with each beam sustaining a different delay.

With the advent of ultrahigh resolution tapped delay lines, equally high-resolution correlators become possible. In Section 3 we exploit this ability to monitor the quality of an optical link with high fidelity and in real time. We also further investigate how impairments to an optical link affect the correlation signal.

### 3. Effect of Impairments on the Correlation Signal

In this section we use simulations to show how various impairments to a fiber optics link, such as attenuation, dispersion, jitter, and noise, affect the shape and amplitude of the correlator's output. We also compare these results with what would be obtained with eye diagrams.

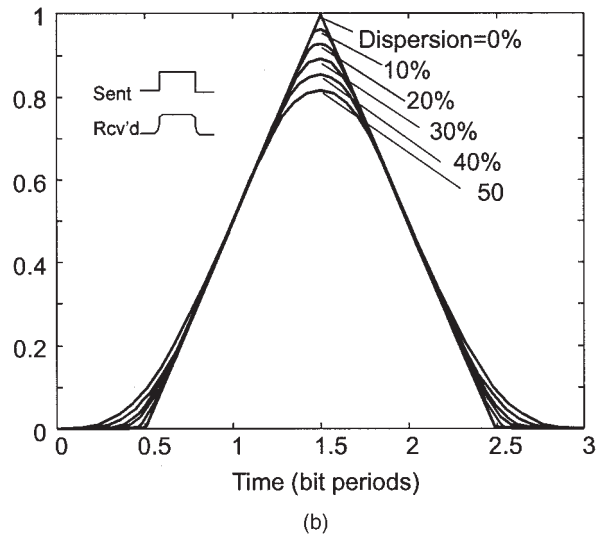
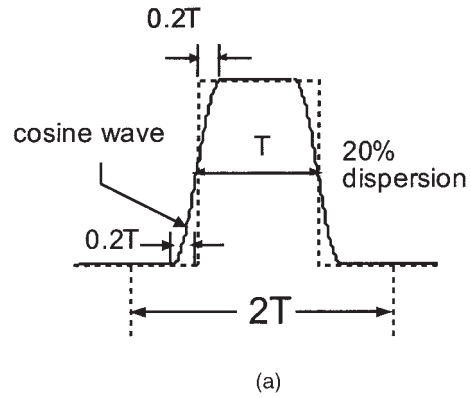


Fig. 5. (a) Dispersion modeled with a cosine wave to make the transitions from 0 to 1 and from 1 to 0. The case for 20% is shown. (b) Effect of dispersion on the correlation signal.

The test signal is 010 and is sampled with 400 samples, each delayed by  $\tau$ . The test signal is artificially impaired by the addition of attenuation, dispersion, and so forth. The degraded signals are then correlated with a crisp, clean 010.

#### A. Effect of Each Impairment Alone on the Correlation Function

Figure 4 shows the resulting correlation functions for received signals subjected to attenuation only. From the figure we see that the height of the correlation peak varies linearly with percent attenuation, measured as percent reduction of the original signal's amplitude, shown in 10% increments.

To model dispersion we took the unattenuated signal mentioned above and modified the sides of the pulse. We used one half cycle of a cosine wave to transition from 0 to 1. We defined percent dispersion as the fraction of the actual bit period occupied by the transition. Figure 5(a) shows the modified bit for a dispersion of 20%. When the dispersion reaches 50%, the rising and falling transitions meet in the middle of the bit. Figure 5(b) shows the effect of dispersion alone on the correlation signal. The

shape and amplitude of the resulting correlation functions are shown for varying amounts of dispersion, ranging from 0% to 50%. Here we see two effects: the amplitude is reduced, and the peak becomes more curved.

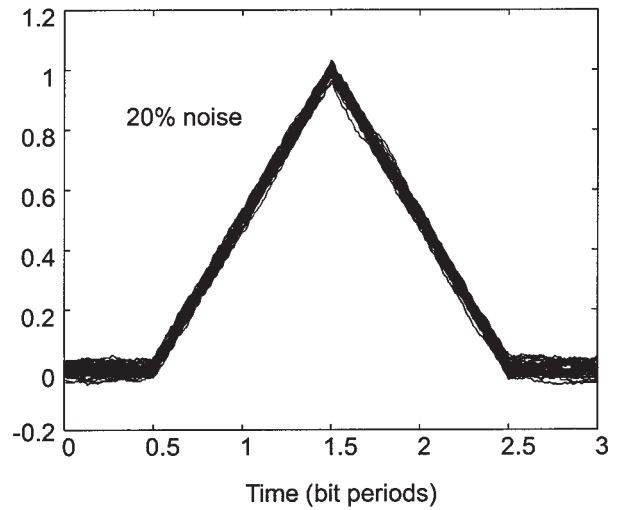
We have seen from Fig. 4 and 5 that information on both attenuation and dispersion can be obtained in a time of  $3T$ . The question is, can one distinguish between them? There are a couple of possibilities. First, suppose one draws a threshold at 50% of the ideal correlation peak. One can observe that, although both attenuation and dispersion produce a reduced peak height and reduced area above this threshold, attenuation produces a narrower peak, whereas dispersion maintains the width but introduces curvature. Thus if one compares the total energy received with the peak height, one can determine the degree to which each effect is present. This requires extra processing time, but even if the signals are converted to electronic ones, the processing time can be on the order of nanoseconds. Another possibility is to perform a second correlation or matched filtering operation to compare the correlation peak with an ideal correlation peak, measuring in effect the degree of curvature. On the other hand, it may not be necessary to distinguish these effects at all, if the goal is only to determine whether the link currently meets some particular quality threshold.

Noise and jitter must be measured statistically over multiple correlations. Noise produces a variation in the peak and slight variations in the shape of the correlation signal. In Fig. 6(a) we vary the amount of noise and examine the average height of the peak and the range of variation. The noise is Gaussian, with a standard deviation of  $\sigma_n$  expressed as a percentage of the bit amplitude (e.g., 10% noise corresponds to noise with  $\sigma = 0.1$  for bits with unit amplitude). For simplicity, the noise is taken here to be the same for both 1's and 0's. Attenuation is not considered in this graph.

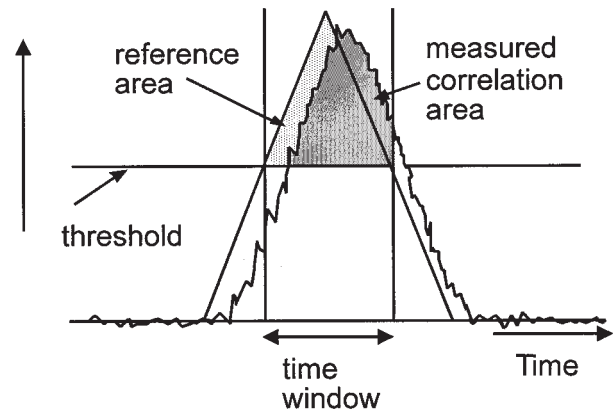
To measure the noise, one might repeat the test signal a hundred or a thousand times and measure the rms variation in the correlation peak height either optically or electronically. Figure 6(a) shows 50 correlation functions superimposed for a 010 test signal with 20% noise ( $\sigma_n = 0.2$ ) added. Noise has the effect of adding both time offset and amplitude variations to the peak.

In practice, it may be easiest to measure the amount of energy received that exceeds some threshold. Figure 6(b) shows this measurement for a signal containing multiple impairments, for an arbitrary threshold of 50%, and for a time window corresponding to the time interval over which an unimpaired signal would exceed 50%. This assumes the existence of some reference clock. Figure 6(c) shows the average correlation peak area received within these reference time and amplitude ranges. In this figure the error bars represent the standard deviation of the excursions as a function of percent noise.

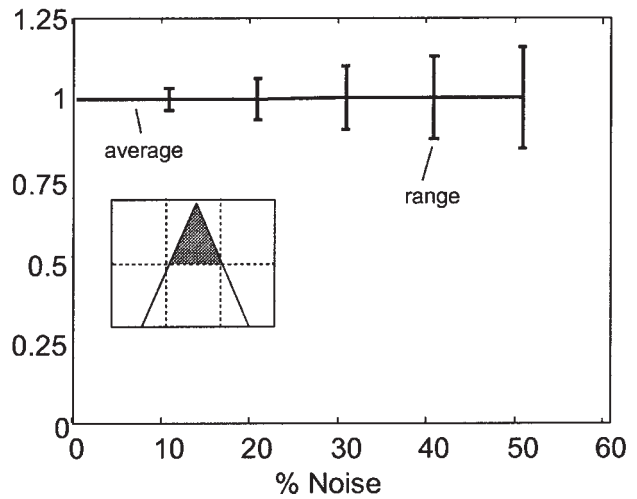
Jitter is modeled here by shifting the received bit



(a)



(b)



(c)

Fig. 6. Effect of noise on correlation function. (a) Fifty separate correlations are superimposed for 20% noise; (b) Measurement of the area of the correlation function that exceeds a certain threshold during a specified time interval; (c) Average and range of the correlation peak area as a function of percent noise.

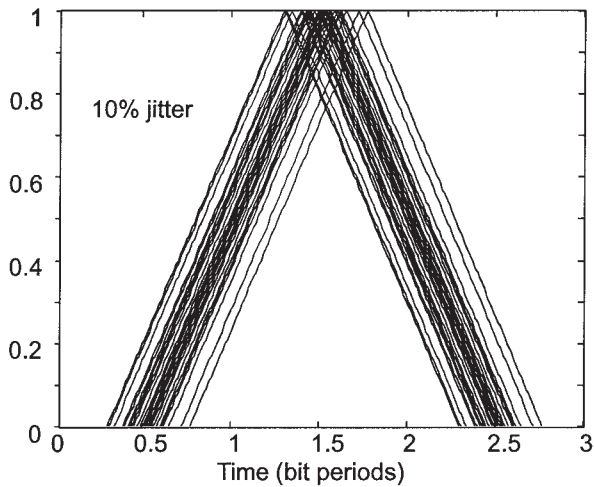


Fig. 7. Fifty superimposed correlations, with jitter varying randomly with standard deviation  $\sigma_j = 10\%$  jitter.

with respect to the reference signal. The result is a correlation function that is also shifted in time, as shown in Fig. 7. For the purposes of simulation, the position of the pulse is shifted by a random number with a standard deviation  $\sigma_j$ , expressed as a fraction of the bit period. As with noise, jitter would be measured over many bits; we have shown 50 correlations superimposed.

So far to develop an understanding of each degradation mechanism affect on the correlation peak, we have considered only the effects of each mechanism alone. Now let us consider what happens when two effects are combined. Figure 8 shows the correlation area as a function of jitter with varying amounts of dispersion. We have again used an amplitude threshold of 50% of the ideal maximum and a time window that corresponds to the case when the ideal

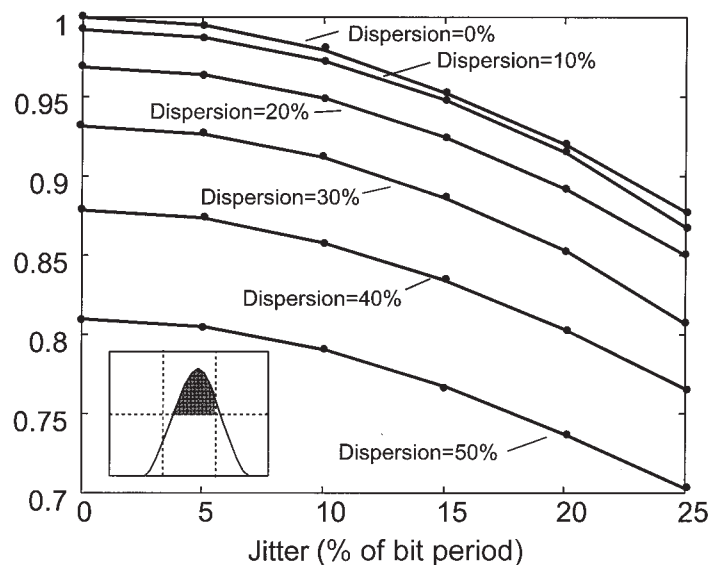


Fig. 8. Area of the correlation function that is greater than the 50% threshold and within the time window in which the ideal correlation function exceeds 50%. The independent variable is jitter, with dispersion as a varying parameter.

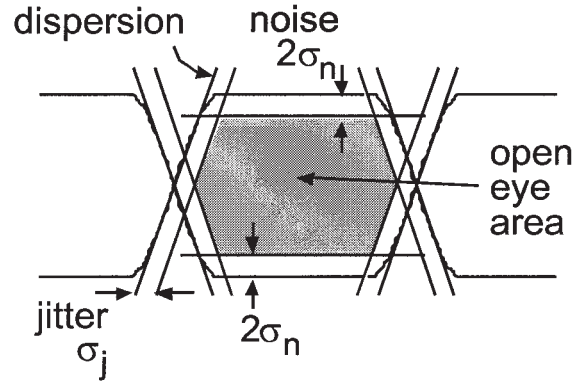


Fig. 9. Simulated eye diagram. The shaded area is the open eye area.

correlation function is greater than 50%. We observe from the figure that the correlation function becomes increasingly sensitive as the impairments become worse for both jitter and dispersion. We also note that the overall area remains fairly high (70% of maximum) even for 50% jitter combined with 50% dispersion. This suggests that the signal-to-noise ratio will remain high even for badly degraded signals.

#### B. Comparison of Correlation and Eye Diagrams

If correlation is to be an effective measure of QoS, then it must relate directly to the quality of the signal as measured by conventional means. We use a simplified eye diagram and compare the open area of the eye with the area of the correlation peak. We do this for various combinations of impairments.

In an eye diagram a long series of bits are superimposed on an oscilloscope. Dispersion clips off the corners of the eyes, jitter narrows the open area (in

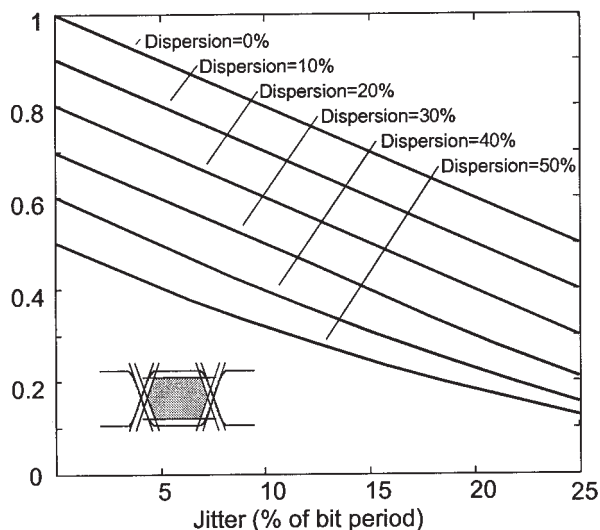


Fig. 10. Variation in the open area of the eye diagram for combined jitter and dispersion. Compare this with the corresponding correlation area of Fig. 8.

time), and noise and attenuation close the eye. The larger the open area, the better the signal. Figure 9 shows a simulated eye diagram. For a particular level of noise  $\sigma$ , expressed as a percentage of the bit amplitude, we draw two lines, one  $2\sigma$  below the "1" level and one  $2\sigma$  above the "0" level. For dispersion, we take a line whose slope is equal to that of our simulated dispersion (see Fig. 5), taking the slope at the point where it crosses 50% amplitude. To include the effects of jitter, we then move these sloping lines toward the inside of the eye by an amount equal to a specified amount of jitter (e.g., 10% of the bit width). We then calculate the area of the eye enclosed by these lines.

Figure 10 shows the eye area calculated by this method for combined jitter and dispersion. This figure can be compared directly with the correlation area of Fig. 8. Both decrease for increasing impairments. We can see that the correlation function area is a reliable indicator of signal impairment and thus bit error rate. The advantages of using correlation are its speed, generating results in a few bit periods instead of in minutes, and no optical-electro-optic conversion.

#### 4. Routing Protocol with the Optical Correlator

Our proposed optical correlator makes it possible to achieve the quality of signal information in real time and to update it as frequently as desired. This functionally has several important applications in all-optical networks, such as routing, testing, protection, and restoration. Here we present a new optical network routing protocol based on the optical correlator.

When discussing routing in an all-optical network, it is usually assumed that all routes have adequate signal quality. This may be ensured by limiting all-optical networks to subnetworks of limited geographic size that are optically isolated from other

parts of the optical layer by transponders. There are, however, strong reasons to consider all-optical networks in which not all routes have adequate signal quality. First, as bit rates increase, it is necessary to increase power. This makes impairments caused by nonlinearities more troublesome. Second, from a supply perspective, optical technology is advancing very rapidly, making ever-larger domains possible. We assume that these considerations will lead to the deployment of a domain of transparency that is too large to ensure that all potential routes have adequate signal quality for all circuits. There is a strong demand in the industry for optical routing protocols that can take into account the impairment effect of an optical layer that degrades signal quality. The optical routing protocol presented here satisfies this requirement.

#### A. Optical Routing Protocol

Here we discuss a quality-based optical routing protocol (QORP). The goal of the QORP is to reduce blocking probability, reduce signaling overhead, and provide quality services to customers. QORP combines intelligent routing with the immediate availability of information about the signal quality provided by the optical correlator.

In QORP the network is divided into domains. Inside each domain the nodes exchange optical link state information, including optical link quality provided by optical correlators. The nodes that are members of more than one domain are called border nodes. In addition to quality information, all nodes receive information about the cost of going through other domains without the need to know the details inside each domain. Each node calculates the path inside its own domain and the domain-wise path to the desired destination. This approach has several advantages. First, it provides each node with the necessary information to make the best routing decision without distributing all the details of the whole network. This reduces the overhead and makes the solution scalable. Second, path selection through domains is based on local, more current information, such as optical link quality, than is currently possible, which leads to more optimized solutions. Third, this solution greatly decreases the load on the network due to flooding and also reduces the database size that each node has to maintain. Fourth, this approach facilitates restoration of broken paths and enables implementations of traffic engineering algorithms.

There are several new aspects to this protocol. First, the optical system impairments are taken into account during the routing process. Second, one can optimize the routing to maximize the revenue generation. This is accomplished by the calculation of path cost, which includes real-time information about the instantaneous link quality provided by the optical correlator and the available bandwidth. Third, a domain-based approach makes the solution scalable and ensures that decisions are made locally based on the most current situation of network resources.

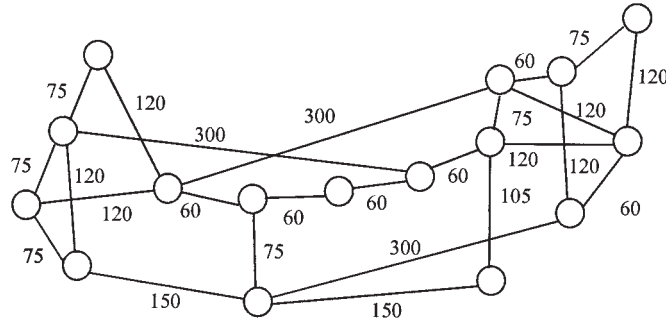


Fig. 11. Topology for self-learning domain-based optical routing protocol. Each domain contains various border nodes (Bs) that exchange information about the quality and cost of each connection.

The protocol is based on an optical link state approach and has the following three behaviors: (1) the optical link state information of the nodes is advertised only within the domain; (2) the border nodes advertise the reachability to other domains inside their domains; and (3) the border nodes aggregate their cost and advertise their updated reachability to other domains after receiving the reachability information from neighboring border nodes. Thus each node has all the information about the actual paths to the border nodes as well as the necessary information about the possible paths to the destination domain. The necessary information for a node includes the average cost and the best signal quality to reach all domains via all border nodes of the given node.

Each node periodically monitors the quality of its links by use of an optical correlator. Based on this information, to establish a path to a destination  $D$  in some other domain, a node computes a number  $k$  of the shortest paths to the destination domain and sends path-probing packets through all those paths. When the nodes in the path receive these packets, they respond by soft reserving the link for the connection and by putting both the cost and the quality of the link in the packet. Thus by receiving these packets, the destination  $D$  is able to find the shortest path of required quality and can then establish the connection and release other paths from the soft-reserved state. Soft reservation is performed to avoid contention for paths in the event that two or more nodes try to establish a connection through the same link.

### 1. Cost and Quality Calculation

The efficiency of the protocol greatly depends on the calculation method of the link cost. In a circuit-switched network, the cost of a link varies considerably just due to a single connection establishment. As soon as a connection is dropped, the cost drops significantly. To capture this, we propose the following function to compute the cost  $C_{L_i}$  of link  $L_i$  for a given connection:

$$C(L_i) = C_{L_{is}} / (AC - N_{L_i}) \quad \text{if } N_{L_i} < AC, \quad (3)$$

where  $AC$  is the number of wavelengths available on all fibers (per link) that connect two adjacent optical

cross connects and  $N_{L_i}$  is the number of occupied (unavailable) wavelengths on link  $L_i$ . The quantity  $C_{L_i}$  is the static cost of the link that is assigned based on various factors, such as distance, number of fibers, availability of optical converters, and possible administrative policies.

The total cost of a path through the network is  $C_p$  and is defined as the summation of the costs of all  $n$  individual links  $L_i$ , spanning the entire source-destination path:

$$C_p = \sum_{i=1}^n C(L_i). \quad (4)$$

The quality of a path is measured in terms of the quality degradation ( $QD_{SD}$ ) and is calculated as follows:

$$QD_p = \sum_{i=1}^n QD(L_i), \quad (5)$$

where  $QD(L_i)$  is the quality degradation of link  $L_i$ , measured by the optical correlator.

Of all the paths computed, the path with least cost and with quality degradation less than a given threshold ( $QD_p < QD_{Th}$ ) is selected for establishing the connection.

### 2. Protocol Simulations

Our proposed optical routing, QORP, has been implemented in Network Simulator (ns-2).<sup>32</sup> A comparison between QORP and an availability-based protocol is performed for the number of calls established that are of acceptable quality. In the availability-based protocol,<sup>2</sup> only the cost of the links is considered in selecting the paths. The National Science Foundation Network (NSF Net), shown in Fig. 11, was used as the topology of the network for our simulations. NSF Net consists of 16 nodes, 25 links, and 128 wavelengths per link. For quality-based routing simulations, some of these links have degraded quality. Traffic is generated between a random source and a destination pair. The number of connections established that satisfies the quality requirements is used as a metric for comparison.

Figure 12 shows the comparison of QORP and the availability-based optical routing protocols when the

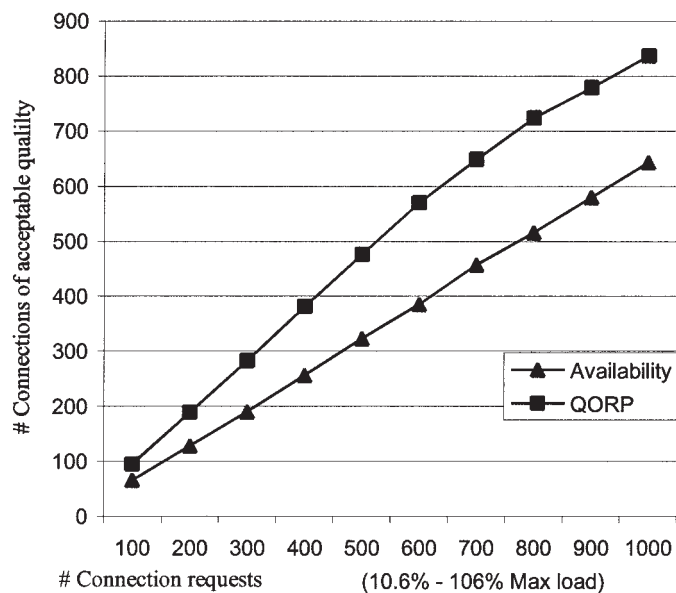


Fig. 12. Comparison of the quality-based (QORP) and the availability-based protocols with a seven-link quality degradation.

quality of seven links has degraded. The number of connections with acceptable quality degradation is plotted against the total number of connection requests. The results show that QORP generates more acceptable connections than that of the availability-based protocol. QORP takes the information provided by the optical correlator into account and establishes calls that are acceptable, whereas the availability-based protocol, which does not account for quality, establishes some calls that are unacceptable. More acceptable calls result in more revenue for service providers and better service for users.

The load offered to the network in our simulations is 100–1000 connection requests (10.6% to 106% of the total load).

### 5. Summary and Conclusion

We have proposed using optical correlation to monitor the health of a fiber-optic or other type of optical network in real time. Optical correlation with very high resolution (hundreds or thousands of samples) is becoming attainable with the advent of improved optical correlators (of the temporal kind), which in turn rely on recent improvements in optical tapped delay lines. To use correlation to monitor the health of a link, one sends a short test message, e.g. 010, subjecting it to whatever impairments the link will impose. At the receiving end, the signal is correlated with an undegraded version of the test signal. The closer the two signals match, the less degradation is imposed by the link and the higher the corresponding correlation signal.

There are two key advantages to monitoring link quality in this manner. One is that the correlation function result is obtained in just 3 bit periods. At 40 Gb/s this corresponds to 75 ps, a significant improvement over the several minutes required with bit error rate or eye diagram measurements. With cor-

relation it becomes feasible for the first time for a network to monitor its own health in real time and to react to changes, decay, or failures in real time.

The other advantage is that the correlation is performed all optically so that conversion to electronics is not necessary, thus reducing the hardware and increasing the speed of the quality-monitoring system.

We showed the effects of various types of impairments, including attenuation, dispersion, noise, and jitter, on the correlation function. We noted that each impairment produces a different effect on the correlation function; thus, it may be possible not only to decide whether a given link meets a given minimum standard of overall quality, but also to perform additional processing to distinguish exactly which link has gone bad.

For a first pass, however, one is likely to simply define some threshold of detectability and issue a go–no signal, either in the optical or the electronic domain. Our simulations that combine dispersion and jitter indicates that the correlation function tracks the open eye area in an eye diagram measurement, verifying that the correlation function does track degradation as measured by more conventional means.

If every node in a network can know the quality of the links to which it is attached and can broadcast that information to other nodes in its domain, then a network can reroute signals based not only on cost or length but also on quality. This enables the service provider to guarantee some standard of quality. Furthermore, if a link degrades enough so that it does not meet some minimum quality standard, then the network can route signals around the bad link, thus restoring the path in real time with a minimum loss of data.

## References

1. B. L. Anderson and R. Mital, "Polynomial-based optical true-time delay devices using MEMs," *Appl. Opt.* **41**, 5449–5461 (2002).
2. C. Assi, A. Shami, M. A. Ali, R. Kurtz, and D. Guo, "Optical networking and real-time provisioning: an integrate visions for the next generation Internet," *IEEE Netw.* **15**, 36–45 (2001).
3. P. H. Ho and H. T. Mouftah, "A novel routing protocol for WDM mesh networks," *Conference on Optical Fiber Communication*, vol. 70 of 2002 OSA Technical Digest Series (Optical Society of America, Washington, D.C., 2002), pp. 38–39.
4. J. Spath, "Dynamic routing strategies for WDM networks," *Computer Networks* (Elsevier, New York, 2000), pp. 523–542.
5. C. F. Hsu, T. L. Liu, and N. F. Huang, "On adaptive routing in wavelength-routed networks," *Opt. Netw. Mag.* **3**(1), 15–24 (2002).
6. J. Strand and A. Chiu, "Impairments and other constraints on optical layer routing," <http://www.ietf.org/internet-drafts/draft-ietf-ipo-impairments-04.txt>. (Internet Engineering Task Force, May 2001), retrieved December 2002.
7. I. Shakei and H. Takara, "Transparent and flexible performance monitoring using amplitude histogram method," *Conference on Optical Fiber Communication*, vol. 70 of 2002 OSA Technical Digest Series (Optical Society of America, Washington, D.C., 2002), pp. 19–21.
8. B. E. A. Saleh and M. C. Teich, *Fundamentals of Photonics* (Wiley, New York, 1991), pp. 868–689.
9. R. A. Sprague and C. L. Koliopoulos, "Time integrating acousto-optic correlator," *Appl. Opt.* **15**, 89–92 (1976).
10. R. J. Berinato, "Acousto-optic tapped delay line filter," *Appl. Opt.* **32**, 5797–5809 (1995).
11. J. Company, J. Cascón, D. Pastor, and B. Ortega, "Reconfigurable fiber-optic delay line filters incorporating electrooptic and electroabsorption modulators," *IEEE Photon. Technol. Lett.* **11**, 1174–1176 (1999).
12. C. T. Chang, J. A. Cassaboom, and H. F. Taylor, "Fibre-optic delay-line devices for R. F. signal processing," *Electron. Lett.* **13**, 678–680 (1977).
13. J. E. Bowers, S. A. Newton, W. V. Sorin, and H. J. Shaw, "Filter response of single-mode fibre recirculating delay lines," *Electron. Lett.* **18**, 110–111 (1982).
14. K. P. Jackson, S. A. Newton, B. Moslehi, M. Tur, C. C. Cutler, J. W. Goodman, and H. J. Shaw, "Optical fiber delay-line signal processing," *IEEE Trans. Microwave Theory Tech.* **MTT-33**, 193–209 (1985).
15. S. A. Newton, K. P. Jackson, and H. J. Shaw, "Optical fiber V-groove transversal filter," *Appl. Phys. Lett.* **43**, 149–151 (1983).
16. G. W. Euliss and R. A. Athale, "Time-integrating correlator based on fiber-optic delay lines," *Opt. Lett.* **19**, 649–651 (1994).
17. A. G. Podoleanu, R. K. Harding, and D. A. Jackson, "Low-cost high-speed multichannel fiber-optic correlator," *Opt. Lett.* **20**, 112–114 (1995).
18. D. M. Gookin and M. H. Berry, "Finite impulse response filter with large dynamic range and high sampling rate," *Appl. Opt.* **29**, 1061–1062 (1990).
19. K.-I. Kitayama, N. Wada, and H. Sotobayashi, "Architectural considerations for photonic IP router based on optical code correlation," *J. Lightwave Technol.* **18**, 1834–1843 (2000).
20. N. Wada and K. Kitayama, "A 10 Gb/s optical code division multiplexing using 9-chip optical bipolar code and coherent detection," *J. Lightwave Technol.* **17**, 1758–1765 (1999).
21. K. Sasayama, M. Okuno, and K. Habara, "Photonic FDM multichannel selector using coherent transversal filter," *J. Lightwave Technol.* **12**, 664–669 (1994).
22. S. P. Wan and Y. Hu, "Two-dimensional optical CDMA differential systems with prime/OOC codes," *IEEE Photon. Technol. Lett.* **13**, 1373–1375 (2001).
23. J. H. Lee, P. C. Teh, P. Petropoulos, M. Ibsen, and D. Richardson, "A grating-based OCDMA coding–decoding system incorporating a nonlinear optical loop mirror for improved code recognition and noise reduction," *J. Lightwave Technol.* **20**, 36–46 (2002).
24. B. Moslehi and J. W. Goodman, "Novel amplified fiber optic recirculating delay line processor," *J. Lightwave Technol.* **10**, 1142–1146 (1992).
25. S. Yegnanarayanan, P. D. Trinh, and B. Jalali, "Recirculating photonic filter: a wavelength-selective time delay for phased-array antennas and wavelength code-division multiple access," *Opt. Lett.* **21**, 740–742 (1996).
26. P. R. Prucnal and M. A. Santoro, "Spread spectrum fiber-optic local area network using optical processing," *J. Lightwave Technol.* **LT-4**, 547–554 (1986).
27. Y. L. Chang and M. E. Marhic, "Fiber-optic ladder networks for inverse decoding coherent CDMA," *J. Lightwave Technol.* **10**, 1952–1062 (1992).
28. B. Moslehi, "Fiber-optic filters employing optical amplifiers to provide design flexibility," *Electron. Lett.* **28**, 226–228 (1992).
29. P. C. Teh, P. Petropoulos, M. Ibsen, and D. J. Richardson, "A comparative study of the performance of seven- and 63-chip optical code-division multiple access encoders and decoders based on superstructured fiber Bragg gratings," *J. Lightwave Technol.* **19**, 1352–1365 (2001).
30. B. L. Anderson and C. D. Liddle, "Optical true-time delay for phased array antennas: demonstration of a quadratic White cell," *Appl. Opt.* **41**, 4912–4921 (2002).
31. A. Rader and B. L. Anderson, "Demonstration of a linear optical true-time delay device using a microelectromechanical mirror array," *Appl. Opt.* **42**, 1409–1416 (2003).
32. Ns-2 is available at <http://www.isi.edu/nsnam/ns/>.